The crystal structure of $MoO_2(O_2)H_2O$

Joel W. Reid,[1,a] James A. Kaduk,[2] and Lidia Matei[3]
[1]*Canadian Light Source, 44 Innovation Boulevard, Saskatoon, SK, Canada, S7N 2V3*
[2]*Illinois Institute of Technology, 3101 S. Dearborn St., Chicago, Illinois, 60616, USA*
[3]*Canadian Isotope Innovations Corp., 232-111 Research Drive, Saskatoon, SK, Canada, S7N 3R2*

(Received 8 November 2017; accepted 2 January 2018)

The crystal structure of $MoO_2(O_2)H_2O$ has been solved by analogy with the $WO_2(O_2)H_2O$ structure and refined with synchrotron powder diffraction data obtained from beamline 08B1-1 at the Canadian Light Source. Rietveld refinement, performed with the software package GSAS, yielded monoclinic lattice parameters of $a = 12.0417(4)$ Å, $b = 3.87003(14)$ Å, $c = 7.38390(24)$ Å, and $\beta = 78.0843(11)°$ ($Z = 4$, space group $P2_1/n$). The structure is composed of double zigzag molybdate chains running parallel to the b-axis. The Rietveld refined structure was compared with density functional theory (DFT) calculations performed with CRYSTAL14, and show strong agreement with the DFT optimized structure. © *2018 International Centre for Diffraction Data*. [doi:10.1017/S0885715618000118]

Key words: molybdenum peroxide, powder diffraction, structure solution, density functional theory

I. INTRODUCTION

New production routes for ^{99}Mo and daughter isotope technetium-99 m (^{99m}Tc), the most widely used radioisotope for medical imaging (Banerjee *et al.*, 2001), are being developed to eliminate the need for expensive nuclear reactors requiring highly enriched uranium and the associated security and nuclear waste concerns (Van Noorden, 2013; Wolterbeek *et al.*, 2014). Emerging methods such as linear accelerator (LINAC) and other accelerator-based production of ^{99}Mo (Galea *et al.*, 2014; Hoedl and Updegraff, 2015) require complementary chemical processes for isotope separation and molybdenum recycling to make these alternative production routes viable (McAlister and Horwitz, 2009; Chattopadhyay *et al.*, 2010; Tkac and Vandergrift, 2016). During the development of target processing and Mo chemical recycling processes, unknown or poorly characterized compounds are sometimes encountered because of the diverse crystal chemistry of molybdenum (Reid *et al.*, 2017). The compound examined in this work was observed during the development of target processing studies for LINAC-based isotope production.

II. EXPERIMENTAL

A specimen of molybdenum processing powder supplied by the Canadian Isotope Innovation Corp. was examined as-synthesized. The specimen was mounted in a 0.3 mm ID Kapton capillary, which was sealed at both ends with adhesive.

Powder X-ray diffraction (PXRD) patterns were collected using a Canadian Macromolecular Crystallography Facility beamline (08B1-1, Fodje *et al.*, 2014) at the Canadian Light Source (CLS). The 08B1-1 is a bending magnet beamline with a Si (111) double crystal monochromator. Two-dimensional (2D) data were obtained using a Rayonix MX300HE detector with an active area of 300 mm × 300 mm. The patterns were collected at an energy of 18 keV ($\lambda = 0.68880$ Å) and a sample-detector distance of 250 mm.

The 2D PXRD patterns were calibrated and integrated using the GSASII software package (Toby and Von Dreele, 2013). The sample-detector distance, detector centering, and tilt were calibrated using a lanthanum hexaboride (LaB6) standard reference material (NIST SRM 660a LaB6) and the calibration parameters were applied to all patterns. After calibration, the 2D patterns were integrated to obtain standard powder diffraction patterns. A pattern collected from an empty Kapton capillary (using the same conditions) was subtracted from the sample data during integration.

Initial search/match phase identification performed with the Powder Diffraction File, PDF-4+ (ICDD, 2016), identified an indexed experimental pattern for H_2MoO_5 (PDF entry 00-041-0359). Subsequent reduced cell searches of the Inorganic Crystal Structure Database (Hellenbrandt, 2004) and the PDF identified a hydrated tungsten peroxide, $WO_2(O_2)H_2O$ [unit cell parameters $a = 12.0710(8)$ Å, $b = 3.8643(2)$ Å, $c = 12.6568(9)$ Å, $\beta = 145.470(3)°$, space group $P2_1/c$], as a potentially analogous structure (ICSD entry 85609, PDF entry 04-011-4400, Pecquenard *et al.*, 1998). The unit cell and structure were transformed from the $P2_1/c$ setting to the $P2_1/n$ setting with an acute β angle for the final Rietveld refinement and DFT optimization.

Rietveld refinement of the crystal structure was performed with the GSAS/EXPGUI programs (Toby, 2001; Larson and Von Dreele, 2004). The pseudo-Voigt reflection profile of Thompson *et al.* (1987) was used, including the asymmetry correction of Finger *et al.* (1994) and the microstrain broadening model of Stephens (1999). Anomalous scattering factors were interpolated from the tables of Sasaki (1989) and input into GSAS. The background was modeled using a three-term Chebyshev polynomial and a nine-term diffuse scattering (Debye) function. Positional parameters were refined with no restraints for the Mo and O atoms, while isotropic

[a]Author to whom correspondence should be addressed. Electronic mail: joel.reid@lightsource.ca

TABLE I. The crystal data, data collection, and refinement parameters obtained for $MoO_2(O_2)(H_2O)$.

Crystal data	
Formula, Z	$MoO_2(O_2)H_2O$, Z = 4
Molecular mass (M_r)	177.97 g mol^{-1}
Symmetry, space group	Monoclinic, $P2_1/n$ (14)
Unit cell parameters	a = 12.0417(4) Å, b = 3.87003(14) Å, c = 7.38390(24) Å, β = 78.0843(11)°
Volume	336.687 (33) Å^3
Density (ρ_{calc})	3.511 g cm^{-3}
Data collection	
Beamline	CLS 08B1-1
Monochromator	Si (111) double crystal monochromator
Detector	Rayonix MX300HE (300 mm × 300 mm)
Specimen mounting	0.3 mm Kapton capillary
Collection mode	Transmission
Wavelength	λ = 0.68880 Å
Collection range, step size	2–39° (2θ), 0.005°/step
Refinement	
Number of data points	7400
Number of reflections	319
Background correction	3-term Chebyshev polynomial, 9-term Debye function
Number of refined parameters	66
R_p	0.0354
R_{wp}	0.0484
R_{exp}	0.0309
χ^2	2.47

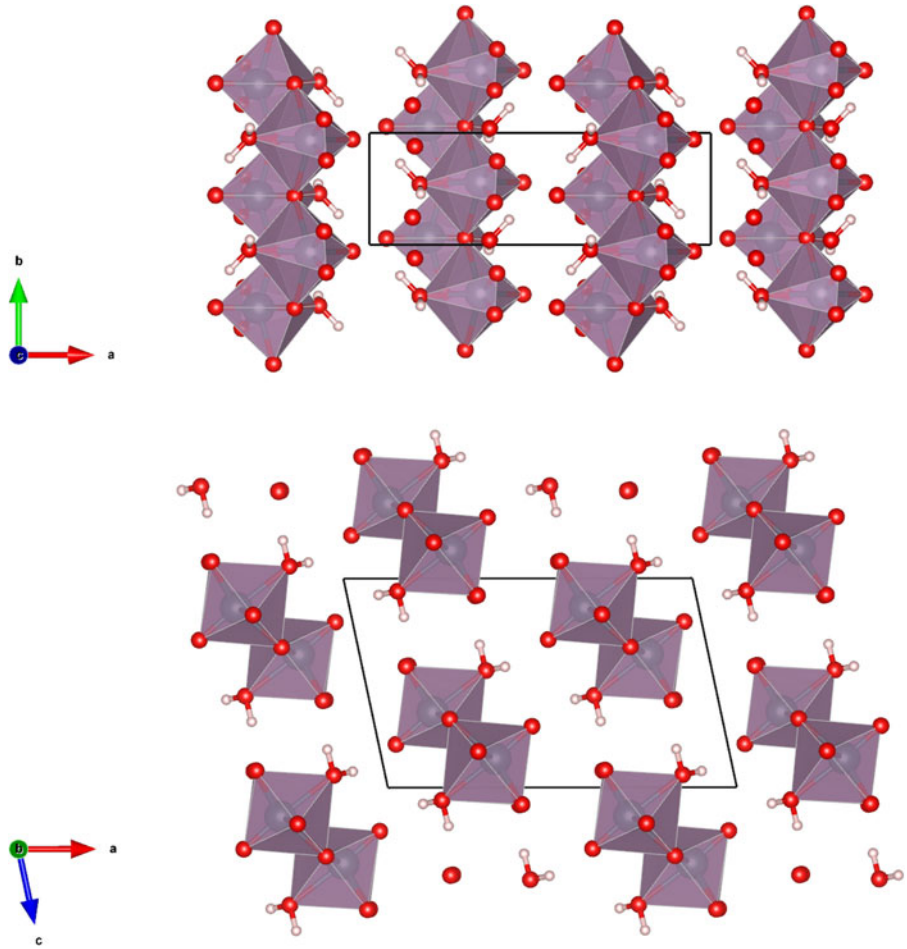

Figure 1. (Colour online) The crystal structure of $MoO_2(O_2)H_2O$, viewed along the c-axis (top) and b-axis (bottom). The polyhedra and atom types can be identified by color including MoO_6 (purple octahedra), hydrogen (pink), and O (red). The unit cell is outlined in black. The figure was prepared with VESTA (Momma and Izumi, 2011).

https://doi.org/10.1017/S0885715618000118 Published online by Cambridge University Press

TABLE II. The Rietveld refined crystal structure of $MoO_2(O_2)H_2O$ with lattice parameters $a = 12.0417(4)$ Å, $b = 3.87003(14)$ Å, $c = 7.38390(24)$ Å, and $\beta = 78.0843(11)°$. All atoms were refined with fixed site occupancies of 1.

Atom	*x/a*	*y/b*	*z/c*	Wyckoff	U_{iso} (Å^2)
Mo1	0.31547(8)	−0.4956(7)	−0.12770(12)	4e	0.01692(34)
O2	0.4430(4)	−0.4257(17)	−0.2982(8)	4e	0.0072(8)
O3	0.2228(4)	−0.484(4)	−0.3303(8)	4e	0.0072(8)
O4	0.3710(7)	−0.6887(26)	0.0777(15)	4e	0.0072(8)
O5	0.3465(8)	−0.3179(27)	0.0863(13)	4e	0.0072(8)
O6	0.14147(35)	−0.5500(20)	0.0557(5)	4e	0.0072(8)
H7	0.09967	−0.32443	0.07484	4e	0.0094(10)
H8	0.15071	−0.54395	0.19135	4e	0.0094(10)

TABLE III. The DFT optimized crystal structure of $MoO_2(O_2)H_2O$ with fixed lattice parameters $a = 12.0432$ Å, $b = 3.8699$ Å, $c = 7.3847$ Å, and $\beta = 78.0960°$.

Atom	*x/a*	*y/b*	*z/c*
Mo1	0.32567	−0.43503	−0.13786
O2	0.45016	−0.44240	−0.29249
O3	0.21910	−0.43717	−0.32737
O4	0.36703	0.38010	0.08299
O5	0.37373	−0.25402	0.08031
O6	0.14773	−0.45755	0.05977
H7	0.09086	−0.27541	0.07774
H8	0.15004	0.45570	0.18310

displacement parameters were refined for the Mo and constrained as equal for all the O atoms. The positions of the H atoms for the water molecule were added late in the refinement based on the results of the DFT calculation, with the isotropic displacement parameter of the H atoms constrained to 1.3 times the value of the O atom. A sixth order spherical harmonic preferred orientation correction (von Dreele, 1997) was refined, yielding a texture index of 1.0232, suggesting limited preferred orientation.

The crystal data, data collection and refinement details are summarized in Table I.

A density functional geometry optimization (using fixed experimental unit cell) was carried out using CRYSTAL14 (Dovesi *et al.*, 2014). The basis sets were obtained from the literature for the H and O (Gatti *et al.*, 1994) and Mo atoms (Cora *et al.*, 1997). The calculation was run on eight 2.1 GHz Xeon cores (each with 6 Gb RAM) of a 304-core Dell

TABLE IV. Mo–O bond lengths obtained from the Rietveld refinement and DFT calculation.

Bond	Rietveld (Å)	DFT (Å)
Mo1–O2	1.794(6)	1.687
Mo1–O3	2.043(5)	2.080
Mo1–O3	1.986(14)	2.047
Mo1–O3	2.070(14)	2.031
Mo1–O4	1.930(9)	1.938
Mo1–O5	1.831(9)	1.951
Mo1–O6	2.257(6)	2.332

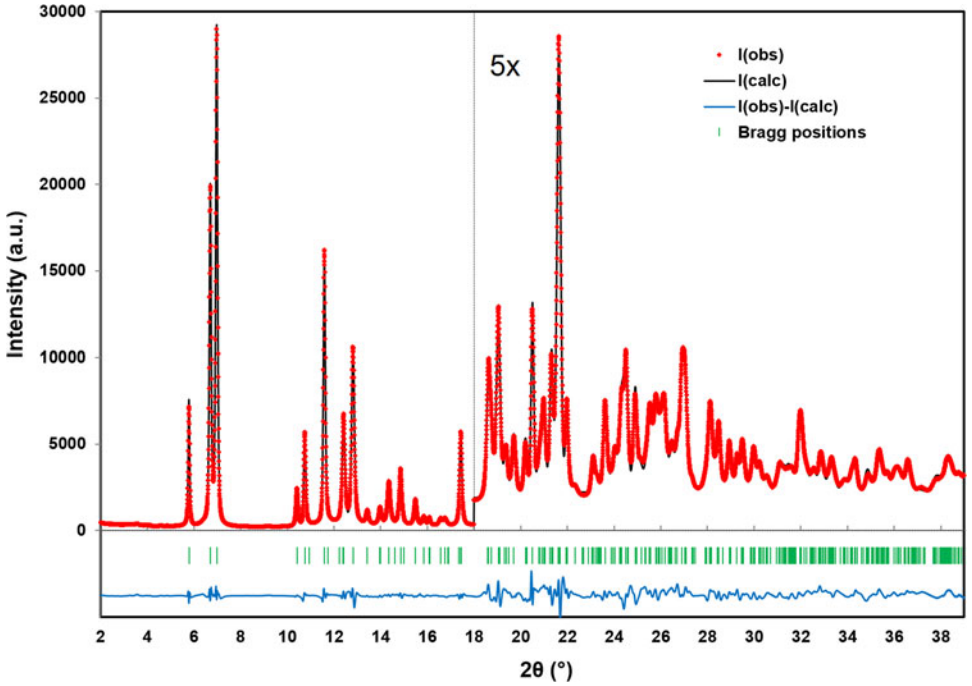

Figure 2. (Colour online) A plot illustrating the final Rietveld refinement of $MoO_2(O_2)H_2O$ obtained with GSAS, zooming in by a factor of 5 for the region above 18° (2θ).

https://doi.org/10.1017/S0885715618000118 Published online by Cambridge University Press

TABLE V. Hydrogen bonds observed in the $MoO_2(O_2)H_2O$ structure and their parameters as determined by the DFT modeling.

H-Bond	D-H (Å)	H···A (Å)	D···A (Å)	D-H···A (°)	Overlap (*e*)	E (kcal mol^{-1})
O6-H8···O5	0.976	1.890	2.857	168.5	0.033	9.9
O6-H8···O4	0.976	2.362	2.916	115.4	0.007	4.6
O6-H7···O2	0.973	1.957	2.859	153.3	0.027	9.0
O6-H7···O2	0.973	2.602	3.197	119.6	0.006	4.2

TABLE VI. The Bragg reflection list obtained from the final Rietveld refinement, prepared by summing reflections closer than 0.02° 2θ as multiple reflections and assigning a weighted average reflection position, then including all reflections with relative integrated intensities of 0.5% or greater up to 35° 2θ.

h	*k*	*L*	d_{calc} (Å)	d_{obs} (Å)	$2\theta_{calc}$ (°)	$2\theta_{obs}$ (°)	I/I_{max} (%)	$\Delta 2\theta$ (°)
1	0	1	6.81830	6.81784	5.791	5.791	20.4	0.000
2	0	0	5.89112	5.89107	6.703	6.703	69.0	0.000
1	0	−1	5.66025	5.65999	6.977	6.977	100.0	0.000
3	0	1	3.79495	3.79486	10.414	10.414	8.2	0.000
1	1	0	3.67677	3.67693	10.749	10.749	19.6	0.000
0	1	1	3.41143	3.41093	11.588	11.590	58.1	−0.002
2	0	2	3.40915	3.41093	11.596	11.590	58.1	0.006
2	1	0	3.23453	3.23464	12.224	12.224	0.5	0.000
1	1	−1	3.19469	3.19481	12.377	12.377	0.5	0.000
3	0	−1	3.18557	3.18558	12.413	12.413	29.3	0.000
2	1	1	3.08550	3.08557	12.817	12.817	49.6	0.000
4	0	0	2.94556	2.94555	13.429	13.429	3.1	0.000
2	0	−2	2.83012	2.83020	13.979	13.979	4.0	0.000
3	1	0	2.75659	2.75663	14.354	14.354	12.7	0.000
1	1	2	2.66405	2.66398	14.856	14.856	15.2	0.000
4	0	2	2.55589	2.55590	15.488	15.488	7.1	0.000
1	1	−2	2.49761	2.49757	15.852	15.852	2.5	0.000
1	0	3	2.46129	2.46087	16.087	16.090	1.9	−0.003
3	1	−1	2.45951	2.46087	16.099	16.090	1.9	0.009
5	0	1	2.39052	2.39048	16.567	16.567	2.1	0.000
3	1	2	2.36277	2.36273	16.763	16.763	2.4	0.000
3	0	3	2.27277	2.27271	17.432	17.432	22.1	0.000
4	1	2	2.13274	2.13273	18.586	18.586	0.6	0.000
4	1	−1	2.12917	2.12921	18.617	18.617	7.1	0.000
5	0	−1	2.11524	2.11525	18.741	18.741	4.3	0.000
4	0	−2	2.08199	2.08200	19.043	19.043	13.2	0.000
3	1	−2	2.05265	2.05264	19.318	19.318	1.6	0.000
0	1	3	2.04469	2.04467	19.394	19.394	1.8	0.000
5	1	0	2.01269	2.01271	19.705	19.705	4.5	0.000
6	0	0	1.96371	1.96369	20.202	20.202	3.5	0.000
0	2	0	1.93502	1.93498	20.505	20.505	10.5	0.000
5	1	2	1.90700	1.90702	20.809	20.809	2.7	0.000
6	0	2	1.89748	1.89746	20.915	20.915	1.4	0.000
5	0	3	1.89069	1.89066	20.991	20.991	4.1	0.000
3	0	−3	1.88675	1.88675	21.035	21.035	0.8	0.000
0	2	1	1.86914	1.86910	21.236	21.236	0.7	0.000
1	2	1	1.86150	1.86147	21.324	21.324	8.1	0.000
4	1	3	1.83731	1.83712	21.608	21.610	18.3	−0.002
2	0	4	1.83639	1.83712	21.619	21.610	18.3	0.009
2	1	−3	1.83460	1.83461	21.640	21.640	5.5	0.000
1	2	−1	1.83098	1.83101	21.683	21.683	9.3	0.000
0	0	4	1.80620	1.80616	21.985	21.985	5.0	0.000
6	1	1	1.77851	1.77853	22.331	22.331	0.6	0.000
7	0	1	1.71961	1.71964	23.106	23.106	2.2	0.000
0	2	2	1.70572	1.70537	23.297	23.302	0.6	−0.005
4	0	4	1.70457	1.70537	23.313	23.302	0.6	0.011
2	2	2	1.68284	1.68281	23.619	23.619	6.8	0.000
1	1	4	1.66414	1.66413	23.888	23.888	0.7	0.000
3.	2	−1	1.65382	1.65383	24.039	24.039	2.7	0.000
5	1	−2	1.63957	1.63958	24.251	24.251	0.5	0.000
2	0	−4	1.63485	1.63447	24.322	24.328	7.4	−0.006
6	1	−1	1.63439	1.63447	24.329	24.328	7.4	0.001
3	1	4	1.62240	1.62239	24.512	24.512	8.4	0.000
2	2	−2	1.59735	1.59737	24.902	24.902	5.3	0.000

Continued

https://doi.org/10.1017/S0885715618000118 Published online by Cambridge University Press

TABLE VI. Continued

h	k	L	d_{calc} (Å)	d_{obs} (Å)	$2\theta_{calc}$ (°)	$2\theta_{obs}$ (°)	I/I_{max} (%)	$\Delta 2\theta$ (°)
6	0	−2	1.59279	1.59277	24.975	24.975	2.3	0.000
1	1	−4	1.58133	1.58131	25.159	25.159	1.2	0.000
7	0	−1	1.56924	1.56922	25.356	25.356	1.0	0.000
6	1	3	1.55946	1.55949	25.517	25.517	5.5	0.000
4	1	−3	1.55670	1.55667	25.563	25.564	1.5	−0.001
7	1	0	1.54351	1.54278	25.786	25.798	7.2	−0.012
4	2	2	1.54275	1.54278	25.799	25.798	7.2	0.001
7	0	3	1.53661	1.53658	25.903	25.904	0.5	−0.001
5	0	−3	1.53343	1.53343	25.958	25.958	1.4	0.000
7	1	2	1.52773	1.52771	26.057	26.057	3.9	0.000
1	2	3	1.52120	1.52117	26.171	26.171	4.7	0.000
5	2	1	1.50403	1.50401	26.475	26.475	3.9	0.000
6	0	4	1.49166	1.49167	26.698	26.698	2.1	0.000
5	1	4	1.48028	1.48030	26.907	26.907	8.4	0.000
3	2	3	1.47335	1.47278	27.036	27.047	7.3	−0.011
8	0	0	1.47278	1.47278	27.047	27.047	7.3	0.000
1	0	5	1.47139	1.47139	27.073	27.073	0.5	0.000
3	0	5	1.45708	1.45708	27.344	27.344	0.5	0.000
5	2	−1	1.42773	1.42775	27.917	27.917	0.8	0.000
3	1	−4	1.41942	1.41943	28.084	28.084	2.5	0.000
4	2	−2	1.41738	1.41735	28.125	28.126	4.2	−0.001
8	1	1	1.40284	1.40284	28.423	28.423	1.6	0.000
1	0	−5	1.39972	1.39971	28.488	28.488	3.9	0.000
2	1	5	1.37879	1.37867	28.929	28.932	3.4	−0.003
6	2	0	1.37829	1.37867	28.940	28.932	3.4	0.008
5	0	5	1.36366	1.36364	29.258	29.258	1.8	0.000
6	2	2	1.35480	1.35481	29.453	29.453	0.5	0.000
0	1	5	1.35368	1.35369	29.478	29.478	2.6	0.000
3	2	−3	1.35087	1.35086	29.541	29.541	0.9	0.000
4	1	5	1.33162	1.33144	29.978	29.982	3.5	−0.004
7	1	−2	1.33122	1.33144	29.987	29.982	3.5	0.005
0	2	4	1.32037	1.32039	30.239	30.239	1.9	0.000
8	1	3	1.30880	1.30881	30.513	30.513	0.9	0.000
7	2	1	1.28539	1.28538	31.083	31.083	2.4	0.000
8	0	4	1.27794	1.27792	31.269	31.269	0.7	−0.001
3	0	−5	1.27355	1.27356	31.379	31.379	0.9	0.000
0	3	1	1.26993	1.26993	31.471	31.471	0.5	0.000
9	0	3	1.26498	1.26499	31.597	31.597	1.1	0.000
7	0	−3	1.26262	1.26262	31.658	31.658	0.6	0.000
2	3	1	1.25080	1.25061	31.965	31.970	5.4	−0.005
9	1	2	1.25042	1.25061	31.975	31.970	5.4	0.005
2	2	−4	1.24881	1.24882	32.017	32.017	1.6	0.000
9	0	−1	1.24389	1.24390	32.147	32.147	1.1	0.000
9	1	0	1.24011	1.24007	32.248	32.249	1.4	−0.001
5	1	−4	1.23996	1.24007	32.252	32.249	1.4	0.003
7	0	5	1.22893	1.22891	32.550	32.550	0.5	0.000
3	3	0	1.22559	1.22558	32.641	32.641	0.8	0.000
1	3	2	1.21712	1.21713	32.874	32.874	3.1	0.000
6	0	−4	1.21065	1.21065	33.055	33.055	0.7	0.000
5	2	−3	1.20181	1.20182	33.305	33.305	1.7	0.000
1	3	−2	1.19999	1.20000	33.357	33.357	1.3	0.000
4	3	1	1.18186	1.18173	33.884	33.888	1.2	−0.004
6	2	4	1.18138	1.18173	33.898	33.888	1.2	0.010
8	2	0	1.17194	1.17193	34.180	34.180	1.3	0.000
1	2	5	1.17124	1.17124	34.201	34.201	0.6	0.000
1	1	6	1.16678	1.16677	34.336	34.336	1.9	0.000
4	3	−1	1.15107	1.15107	34.819	34.819	0.5	0.000

Linux cluster at the Illinois Institute of Technology (IIT), used 8 k-points and the B3LYP functional, and took less than 1 day.

III. RESULTS AND DISCUSSION

Figure 1 illustrates the DFT optimized structure from two views along the *c*-axis and the *b*-axis, while the Rietveld refined and DFT optimized atomic coordinates are given in Tables II and III, respectively. The final Rietveld refinement, yielding a reduced χ^2 value of 2.47, is illustrated in Figure 2. The root-mean-square Cartesian displacement between the Rietveld refined and DFT optimized structures for the heavy (non-hydrogen) atoms is 0.1330 Å, well within a reasonable range for correct crystal structures. The largest

https://doi.org/10.1017/S0885715618000118 Published online by Cambridge University Press

peak and hole in the difference Fourier map were 0.513 e $Å^{-3}$ (at two locations; 0.49 Å from Mo1 and 1.15 Å from O3) and −0.480 e $Å^{-3}$ (between adjacent molybdate chains, 1.77 Å from O2) respectively.

The crystal structure is characterized by double zigzag molybdate chains running parallel to the *b*-axis, where adjacent molybdate octahedra share edges and a corner of each octahedron has been replaced by a peroxo ligand oriented nearly parallel the *b*-axis. The octahedra are distorted and the Mo–O bond lengths obtained from both the Rietveld refinement and the DFT optimization are given in Table IV. The bond valence sum (Brown, 2002) values for Mo1 are 6.057(60) and 5.954 for the Rietveld refined and DFT optimized structures, respectively. Hydrogen bonds based on the DFT optimized structure are shown in Table V. Both hydrogen bonds through H8 connect to a single adjacent molybdate chain with the peroxo ligand oxygen atoms (O4 and O5) as acceptors. One hydrogen bond through H7 connects to a second adjacent molybdate chain (via O2 as an acceptor), while the second bond is within the same chain.

A Bragg reflection list, shown in Table VI, was prepared by summing reflections closer than 0.02° (2θ) as multiple reflections and assigning a weighted average reflection position, then including all reflections with relative integrated intensities of 0.5% or greater up to 35° (2θ). The Bragg reflection list and raw data are contained in a crystallographic information file (CIF) in the online Supplementary material. Individual CIF files containing the Rietveld refined and DFT calculated structures are also included as Supplementary material.

SUPPLEMENTARY MATERIAL

The supplementary material for this article can be found at https://doi.org/10.1017/S0885715618000118

ACKNOWLEDGEMENTS

The authors thank Andrey Rogachev for the use of the computing resources at the Illinois Institute of Technology. Research described in this paper was performed using beamline 08B1-1 at the Canadian Light Source, which is supported by the Canadian Foundation for Innovation, the Natural Sciences and Engineering Research Council of Canada, the National Research Council Canada, the Canadian Institutes of Health Research, the Government of Saskatchewan, Western Economic Diversification Canada, and the University of Saskatchewan.

Banerjee, S., Pillai, M. R. A., and Ramamoorthy, N. (**2001**). "Evolution of Tc-99 m in diagnostic radiopharmaceuticals," Semin. Nucl. Med. **31**, 260–277.

Brown, I. D. (**2002**). *The Chemical Bond in Inorganic Chemistry: The Bond Valence Model* (Oxford University Press, New York).

Chattopadhyay, S., Das, S. S., and Barua, L. (**2010**), "A simple and rapid technique for recovery of ^{99m}Tc from low specific activity (n,γ)^{99}Mo based on solid–liquid extraction and column chromatography methodologies," Nucl. Med. Biol. **37**, 17–20.

Cora, F., Patel, A., Harrison, N. M., Roetti, C., and Catlow, C. R. A. (**1997**). "An ab-initio Hartree-Fock study of alpha-MoO_3," J. Mater. Chem. **7**, 959–967.

Dovesi, R., Orlando, R., Erba, A., Zicovich-Wilson, C. M., Civalleri, B., Casassa, S., Maschio, L., Ferrabone, M., De La Pierre, M., D'Arco, P., Noel, Y., Causa, M., Rerat, M., and Kirtman, B. (**2014**). "CRYSTAL14: a program for the *Ab initio* investigation of crystalline solids," Int. J. Quantum Chem. **114**, 1287–1313.

Finger, L. W., Cox, D. E., and Jephcoat, A. P. (**1994**). "A correction for powder diffraction peak asymmetry due to axial divergence," J. Appl. Crystallogr. **27**, 892–900.

Fodje, M., Grochulski, P., Janzen, K., Labiuk, S., Gorin, J., and Berg, R. (**2014**). "08B1-1: an automated beamline for macromolecular crystallography experiments at the Canadian Light Source," J. Synchrotron Radiat. **21**, 633–637.

Galea, R., Ross, C., and Wells, R. G. (**2014**). "Reduce, reuse and recycle: a green solution to Canada's medical isotope shortage," Appl. Radiat. Isot. **87**, 148–151.

Gatti, C., Saunders, V. R., and Roetti, C. (**1994**). "Crystal-field effects on the topological properties of the electron-density in molecular crystals – the case of urea," J. Chem. Phys. **101**, 10686–10696.

Hellenbrandt, M. (**2004**). "The Inorganic Crystal Structure Database (ICSD) – present and future," Crystallogr. Rev. **10**, 17–22.

Hoedl, S. A. and Updegraff, W. D. (**2015**). "The production of medical isotopes without nuclear reactors or uranium enrichment," Sci. Glob. Sec. **23**, 121–153.

ICDD (**2016**), PDF-4+ 2016 (Database). International Centre for Diffraction Data, edited by Dr. Soorya Kabekkodu (Newtown Square, PA, USA).

Larson, A. C. and Von Dreele, R. B. (**2004**). *General Structure Analysis System (GSAS)* (Report No. LAUR 86-748). Los Alamos, NM: Los Alamos National Laboratory.

McAlister, D. R. and Horwitz, E. P. (**2009**). "Automated two column generator system for medical radionuclides," Appl. Radiat. Isot. **67**, 1985–1991.

Momma, K. and Izumi, F. (**2011**). "VESTA 3 for three-dimensional visualization of crystal, volumetric and morphology data," J. Appl. Crystallogr. **44**, 1272–1276.

Pecquenard, B., Castro-Garcia, S., Livage, J., Zavalij, P. Y., Whittingham, M. S., and Thouvenot, R. (**1998**). "Structure of hydrated tungsten peroxides $[WO_2(O_2)H_2O]\cdot nH_2O$," Chem. Mater. **10**, 1882–1888.

Reid, J. W., Kaduk, J. A., and Olson, J. A. (**2017**). "The crystal structure of $Na(NH_4)Mo_3O_{10}\cdot H_2O$," Powder Diffr. **32**, 140–147.

Sasaki, S. (**1989**). *Numerical Tables of Anomalous Scattering Factors Calculated by the Cromer and Lieberman's Method* (KEK–88-14). Japan.

Stephens, P. W. (**1999**). "Phenomenological model of anisotropic peak broadening in powder diffraction," J. Appl. Crystallogr. **32**, 281–289.

Thompson, P., Cox, D. E., and Hastings, J. B. (**1987**). Rietveld refinement of Debye-Scherrer synchrotron X-ray data from $A1_20_3$," J. Appl. Crystallogr. **20**, 79–83.

Tkac, P and Vandergrift, G. F. (**2016**). "Recycling of enriched Mo targets for economic production of ^{99}Mo/^{99m}Tc medical isotope without use of enriched uranium," J. Radioanal. Nucl. Chem. **308**, 205–212.

Toby, B. H. (**2001**). "EXPGUI, a graphical user interface for GSAS," J. Appl. Crystallogr. **34**, 210–213.

Toby, B. H. and Von Dreele, R. B. (**2013**). "GSAS II: the genesis of a modern open-source all-purpose crystallography software package," J. Appl. Crystallogr. **46**, 544–549.

Van Noorden, R. (**2013**). "The medical testing crisis," Nature **504**, 202–204.

Von Dreele, R. (**1997**). "Quantitative texture analysis by Rietveld refinement," J. Appl. Crystallogr. **30**, 517–525.

Wolterbeek, B., Kloosterman, J. L., Lathouwers, D., Rohde, M, Winkelman, A., Frima, L., and Wols, F. (**2014**). "What is wise in the production of ^{99}Mo? A comparison of eight possible production routes," J. Radioanal. Nucl. Chem. **302**, 773–779.